Protein Engineering vol.13 no.2 pp.133–141, 2000

Structural characterization of protein–denaturant interactions: crystal structures of hen egg-white lysozyme in complex with DMSO and guanidinium chloride

Shekhar C.Mande[1] and M.Elizabeth Sobhia[2]

Institute of Microbial Technology, Sector 39-A, Chandigarh 160 036, India

[1]To whom correspondence should be addressed
Email: shekhar@bragg.imtech.ernet.in

[2]Present address: National Institute of Pharmaceutical Education and Research, SAS Nagar, Punjab, India

A variety of physico-chemical methods employ chemical denaturants to unfold proteins, and study different biophysical processes involved therein. Chemical denaturants are believed to induce unfolding by stabilizing the unfolded state of proteins over the folded state, either macroscopically or through specific interactions. In order to characterize the nature of specific interactions between proteins and denaturants, we have solved crystal structures of hen egg-white lysozyme complexed with denaturants, and report here dimethyl sulfoxide and guanidinium chloride complexes. The dimethyl sulfoxide molecules and guanidinium ions were seen to bind the protein at specific sites and were involved in characteristic interactions. They share a major binding site between them, the C site in the sugar binding cleft of the enzyme. Although the overall conformations of the complexes were very similar to the native structure, spectacular conformational changes were seen to occur locally. Temperature factors were also seen to drop dramatically in the local regions close to the denaturant binding sites. An interesting observation of the present study was the generation of a sodium ion binding site in hen egg-white lysozyme in the presence of denaturants, which was hitherto unknown in any of the other lysozyme structures solved so far. Loss of some of the crucial side chain–main chain interactions may form the initial events in lysozyme unfolding.

Keywords: denaturant/DMSO/guanidine chloride/hen egg-white lysozyme/sodium ion

Introduction

Chemical denaturation of proteins is frequently used as a model technique to understand various aspects of protein folding. Among many others, such studies give insights into the stability of proteins, nature of their unfolded state, folding pathways, etc. The denaturants serve as a useful tool to address these important questions, although whether one can extrapolate direct conclusions from these studies to *in-vivo* situations remains a topic of considerable debate. Some of the commonly used denaturants, such as urea, guanidinium chloride (GnCl), dimethyl sulfoxide (DMSO), etc., are believed to unfold proteins by interfering with the molecular interactions that stabilize the folded form of proteins (Thayer *et al*., 1993). A detailed molecular view of how the denaturants may actually induce unfolding of proteins is however yet to emerge.

Although a significant amount of work has been carried out in the past on protein co-solvent interactions (Buck, 1998), it is uncertain at present whether the effect of denaturants on proteins can be described as ligand binding (Tanford, 1968), or alternatively can be depicted as a macroscopic phenomenon (Breslow and Guo, 1990). Evidence for the former has been presented through crystallographic and calorimetric studies (Makhatadze and Privalov, 1992; Thayer *et al*., 1993), while the latter has been suggested by studying solvent behaviour in high concentrations of denaturants (Breslow and Guo, 1990). X-Ray crystallography offers itself as a useful technique to address these questions if unfolding is described through the protein–ligand interaction model. Although it may be impossible to crystallize proteins in their denatured state due to the inherent conformational heterogeneity, efforts are consistently being made to visualize protein–denaturant interactions at the onset of the denaturation process (Pike and Acharya, 1994; Dunbar *et al*., 1997; Ratnaparkhi and Varadarajan, 1997).

Hen egg-white lysozyme (HEWL) is an attractive protein to address structural questions due its large availability and ease of crystallization. Crystallographic structures of HEWL have been utilized in the past to understand several chemical and biophysical effects on protein structure; for instance, effect of high pressure (Kundrot and Richards, 1987), effect of low temperatures (Young *et al*., 1994), effect of low environmental humidity (Kodandapani *et al*., 1990) and interaction of dyes and other organic compounds with proteins (Lehmann *et al*., 1985; Madhusudan and Vijayan, 1992; Liepinsh and Otting, 1997; Buck, 1998), etc. It is therefore no surprise that the earliest studies of visualization of interaction between denaturants and proteins were also done using HEWL as the model protein (Snape *et al*., 1974).

Apart from the extensive knowledge gained using its structure, HEWL has also been a model protein of choice for several physico-chemical studies related to protein folding. Many experimental and theoretical studies carried out on HEWL have yielded answers to the nature of its collapsed state, pathways undertaken to achieve the final folded form and the late stages of protein folding (Dobson *et al.*, 1994). These studies have indicated that the final packing of side chains and the sacrifice in conformational entropy is achieved only in the final stages of folding of HEWL. Thus, an important lesson from these studies has been that the rate of folding appears to be limited by the rearrangements of native-like conformational states to the native structure, rather than exploring the entire conformational space available for the polypeptide to the fold (Dobson *et al*., 1994). We therefore chose HEWL as a model to study protein–denaturant interactions, and report here its complexes with DMSO and GnCl.

Materials and methods

Crystallizations

Hen egg-white lysozyme, obtained commercially from Sigma, was crystallized using minor modifications of the well known

Table I. Crystal parameters and data collection statistics

	DMSO complex	GnCl complex
a	79.5	79.4
b	79.5	79.4
c	37.9	37.8
Maximum resolution (Å)	2.2	2.2
Overall R_{merge}	0.110	0.095
R_{merge} last shell (2.28–2.2 Å)	0.271	0.267
Overall completeness (%)	99.6	93.2
Completeness last shell (2.28–2.2 Å) (%)	100	96.8

Space group of both the complexes is $P4_32_12$.

conditions in the tetragonal form (Alderton *et al*., 1945). During the hanging drop crystallizations, denaturant solutions were added to the protein drop in increasing concentrations, enabling the denaturants to co-crystallize along with the protein. For the DMSO–lysozyme co-crystals, crystals could not be obtained beyond 20% (v/v) concentration of DMSO. Similarly, for the GnCl–lysozyme complex, crystals could not be obtained in excess of 1.2 M GnCl. The best crystals in complex with DMSO were obtained using 0.1 M acetate buffer at pH 4.6, 16% NaCl and 20% DMSO. The complex crystals of GnCl and lysozyme were obtained under the optimal conditions of 0.1 M acetate buffer, 12 % NaCl and 1.2 M GnCl.

Data collection and processing

Three-dimensional diffraction data were collected using an MAR imaging plate mounted on a Rigaku rotating anode X-ray generator. The crystal to film distance was maintained at 150 mm throughout the data collection. Crystals were exposed to X-rays in an unknown orientation, which was later identified by autoindexing. Diffraction data were processed using HKL/DENZO suite of programs, and scaled using SCALEPACK (Otwinowski and Minor, 1997). The final data collection statistics are shown in Table I. The data are 100 and 93.2% complete to 2.2 Å resolution for the DMSO and GnCl complexes respectively.

Refinement and identification of DMSO and guanidinium positions

Since the crystals did not show large variations in cell dimensions from the native form, refinement could be initiated without the need of structure solution through molecular replacement. HEW lysozyme structure refined at 2.0 Å resolution (PDB code 2LYM; Kundrot and Richards, 1989) was chosen as the starting set of coordinates. Water molecules in the initial model were not considered. Program REFMAC (Murshudov *et al*., 1997) in the CCP4 suite of programs (CCP4, 1994) was used to refine the coordinates. Restrained refinement was carried out using a target maximum likelihood function. Five percent of the total data were set aside for the calculation of R_{free} to monitor the progress of refinement. Model building and electron density examination was carried out on a Silicon Graphics Indigo^2 workstation, using the O program (Jones *et al*., 1991).

In the initial stages of refinement, the largest peaks in the difference Fourier maps were assigned water positions if the corresponding density did not appear to be large enough to accommodate a DMSO molecule or appear planar to accommodate a guanidinium (Gnd) ion. Distance from the centre of the difference electron density to the nearest polar atom was also checked to further verify if the density did indeed correspond to a water molecule. If this distance was greater than 3.5 Å, it was not assigned a water position. The densities for DMSO as well as Gnd ions was modelled only after a careful inclusion of water molecules. The quality of the refined structure was assessed using various geometric criteria as available in the program PROCHECK (Laskowski *et al*., 1993).

Table II. The final refinement statistics

	DMSO complex	GnCl complex
Number of reflections used in refinement	6226	5803
Number of reflections for evaluation of R_{free}	302	284
Resolution (Å)	31.5–2.2	39.7–2.2
Number of atoms:		
protein	1014	1001
water	63	64
sodium ion	1	1
denaturant	8	8
Final R	0.187	0.191
Final R_{free}	0.260	0.264
Average B (Å^2):		
main chain	26.1	20.1
side chain	30.7	23.6
water	40.0	31.7
sodium ion	31.0	13.3
denaturant	42.2	36.0

Results

Crystallizations and data collection

Crystallizations were set up with the aim of obtaining suitable crystals with maximum permissible concentration of the denaturants. Although the crystallizations were set up with increasing concentrations of DMSO and GnCl, good crystals could be obtained only up to 20% (v/v) DMSO and 1.2 M GnCl concentrations. At these concentrations of denaturants, the activity of lysozyme is not known to be disrupted. However, beyond these concentrations of the denaturants, crystals were either too small, or were not useful for diffraction purposes. Moreover, the crystals showed a poorer diffraction compared with the native lysozyme, which is known to diffract to at least 1.8 Å resolution under similar conditions. Both the DMSO as well as GnCl complex crystals diffracted only up to 2.2 Å resolution. The crystal and diffraction data statistics are shown in Table I. Merging R-factors including all reflections for the DMSO and GnCl data sets were 0.11 and 0.095, respectively.

Progress of refinement and identification of solvent positions

X-Ray refinement of both the complexes was initiated with the native structure without consideration of water molecules. The starting R and R_{free} were 0.277 and 0.280, respectively, for DMSO and 0.300 and 0.294 for the GnCl complexes. The final refinement statistics are shown in Table II. The geometry of the final models was very good as judged by the PROCHECK program (Laskowski *et al*., 1993), with approximately 88% residues falling within the most favoured regions of the respective Ramachandran plots (data not shown).

Examination of difference Fourier maps revealed a main chain disorder at residues Arg73 and Asn74 in the DMSO complex. The two residues, Arg73 and Asn74, in the DMSO complex were therefore modelled in two alternate conformations. Interestingly, in the GnCl complex the same residues

were involved in a main chain peptide flip, thus giving an opposite orientation to the Arg73 carbonyl oxygen. A similar flip has been observed earlier in the urea complex with lysozyme (Pike and Acharya, 1994). We strongly believe that the disorder in residues Arg73–Asn74 in the DMSO complex is a result of a dynamical behaviour rather than a static positional disorder due to its inclination for flipping.

Major considerations for modelling the DMSO and Gnd densities were based on shapes of the respective molecules in difference electron density maps. Moreover, before modelling the DMSO and Gnd ions, it was ensured that the centre of difference electron density was farther than 3.5 Å from the closest polar atom of the protein, or a nearby water, thus ruling out misinterpretation of a water, or a buffer molecule to be a denaturant molecule. The DMSO molecules could be identified unambiguously in the density due to their characteristic shape. Electron density for both the DMSO molecules exhibited a distinct asymmetric bulge, making placement of the sulfur atom easier. Thus, the sulfur atom position was assigned to the highest electron density in this protrusion. There was, however, difficulty in positioning the oxygen and the two carbons of DMSO since there could be three possible orientation of DMSO in the density. The final orientation was decided upon with the consideration of involvement in hydrogen bonding of its oxygen atom. With these criteria, two positions each of the DMSO and Gnd molecules were identified in the respective complexes. Typical electron densities for the denaturant molecules are shown in Figure 1. In addition to identifying positions of the solvent atoms, a strong density was attributed to a sodium ion, based on its octahedral coordination (Figure 2). The final model of the DMSO complex therefore contained 1014 protein atoms including 13 atoms in alternate conformation, 63 waters, one sodium ion and eight atoms of two DMSO molecules. Similarly, the GnCl complex structure contained 1001 protein atoms, 64 waters, one sodium ion and eight atoms belonging to two Gnd ions.

Interaction of DMSO and guanidinium ions with lysozyme

As mentioned in the preceding paragraphs, there are two DMSO binding sites in the HEW lysozyme–DMSO complex structure (Figures 3a and b). The primary binding site occupies the C-subsite in the binding cleft of lysozyme and is formed by residues Trp63, Asn59, Ile98, Ala107 and Trp108 (Figure 3a). The oxygen atom of the DMSO forms a bifurcated hydrogen bond with the main chain N of Asn59 and $N^{\varepsilon 1}$ of Trp63. The sulfur atom position, which could not be located in the neutron diffraction experiments (Lehmann and Stansfield, 1989), unambiguously points away from the protein moiety. There are extensive van der Waal's contacts between the DMSO molecule and residues mentioned above. The binding of DMSO at this site is identical to that found by neutron diffraction experiments (Lehmann and Stansfield, 1989) with the sulfur atom pointing farther away from the protein moiety. At the second site, the DMSO molecule is embedded in a small depression on the surface of lysozyme (Figure 3b). This binding site is primarily formed by the side chains of Asp119, Gln121, Ala122 and Arg125. The oxygen atom of the DMSO molecule is involved in hydrogen bonding with the guanidinyl nitrogen of Arg125. Temperature factors of the second DMSO molecule (47 $Å^2$) were higher than the first one (37.4 $Å^2$). Similar to the primary DMSO molecule, the second molecule also forms extensive van der Waal's contacts with the side chains mentioned above.

There are two Gnd ions found in the HEWL–GnCl structure, as mentioned earlier (Figure 4a and b). Both the Gnd ions are involved in extensive hydrogen bonding/ionic interactions. One of the Gnd ions (Gnd1) occupies the same position as that of the primary DMSO molecule in the C-subsite of the enzyme. Binding of this Gnd ion mimics binding of the acetamido group of *N*-acetyl sugars in the GlcNAc complexes with similar chemical interactions (Cheetham *et al*., 1992). This Gnd ion additionally interplays interestingly with Trp108 forming unique interactions with the π electrons of its side chain as shown in Figure 4a. These interactions are reminiscent of the weakly polar interactions observed in protein structures (Burley and Petsko, 1988). It also hydrogen bonds with the main chain N of Asn59 and the carbonyl oxygen of Ala107. One of the three nitrogens of the Gnd ion interacts with $N^{\varepsilon 1}$ of Trp63 through a bridging water molecule. Similar water mediated interaction is also exhibited by the other Gnd ion, where its two nitrogen atoms are involved in interactions with Arg14 (Figure 4b). The second Gnd ion interacts with the side chain of His15, and main chain nitrogen of Ile88. Thus, all the nitrogen atoms of the two Gnd ions are involved in extensive hydrogen bonding interactions, both donating as well as accepting hydrogen bonds from the protein atoms. Temperature factors of the two Gnd ions are 35.6 and 36.4 $Å^2$.

When compared with the native lysozyme structure in the primary binding site, i.e. in the C-subsite, the Gnd ion as well as the DMSO molecule are seen to replace two water molecules. In the second binding site, the Gnd ion once again replaces two water molecules, while the second DMSO molecule replaces one bound water of the native lysozyme.

Comparison of conformational features of the two complexes with native lysozyme

The overall conformations of the two complexes were very similar to the native lysozyme, as anticipated. The r.m.s. difference calculated using all the main chain as well as side chain coordinates, when the respective complexes were superimposed with the native lysozyme, were 0.33 and 0.39 Å for the DMSO and Gnd complex structures respectively (Figure 5a and b). The r.m.s. displacement in temperature factors was 11.7 and 9.1 $Å^2$, respectively, for the two complexes when compared with the native structure. At residues 73 and 74, the temperature factors dropped dramatically when compared to the native structure (Figure 6a and b). The drop in temperature factors is significant for the side chains of residues 73 and 74, although the main chain also shows notable ordering. Side chains involved in interactions with denaturant molecules also show improvement in B-factors, reinforcing the interpretation of the denaturant positions.

The most spectacular conformational change that takes place in the denaturant complexes relates to the peptide flip at residue 73. The peptide flips only partially in the DMSO complex, where it has been modelled with an alternate conformation. Both the conformations are likely to have approximately equal occupancies since they refine to similar B values. The flip, however, appears to be complete in the GnCl complex, where we did not find any trace density for the possible alternate conformation in the difference Fourier maps. The peptide flip results in a change of almost 180° in the main chain ψ angle of residue Arg73. The [ϕ] and ψ angles of residue 73 in the native structure were -100 and -10, respectively, while these were respectively -101 and 162 in the DMSO complex, and -106 and 162 in the GnCl complex.

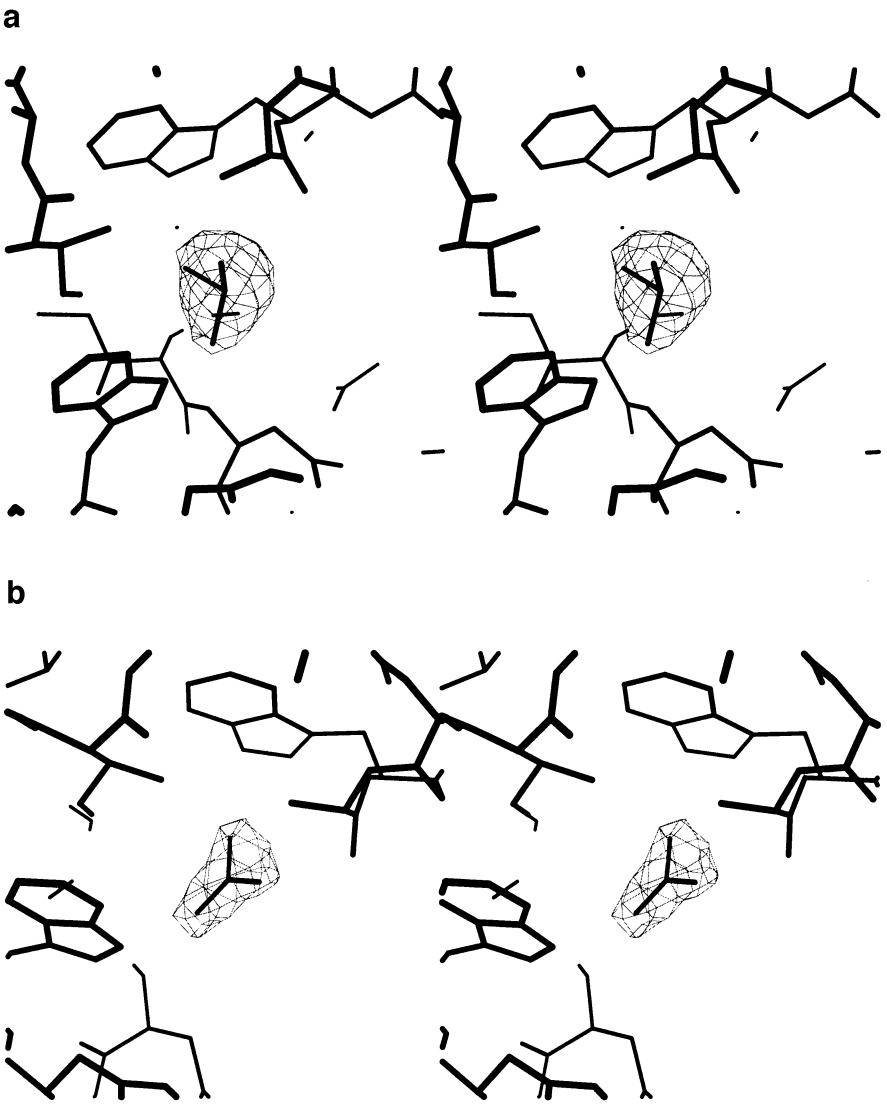

Fig. 1. Stereo view of (**a**) DMSO and (**b**) GnCl electron density at the C-site in the lysozyme cleft. The electron density is plotted at 2σ above the mean level in the F_o—F_c map.

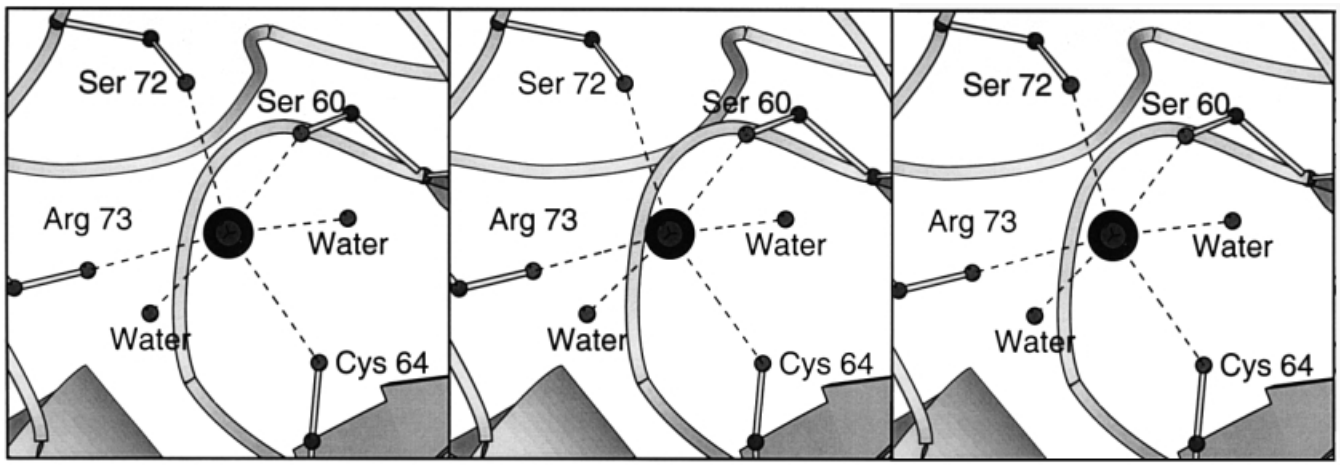

Fig. 2. Stereo view of the sodium ion binding site. The binding site geometry is identical in both the complexes. In the DMSO complex, however, due to a disorder in the Arg73—Asn74 residues, and a missing water molecule, the sodium ion is only partially occupied. This figure, as well as Figures 3 and 4, were produced using MOLSCRIPT (Kraulis, 1991).

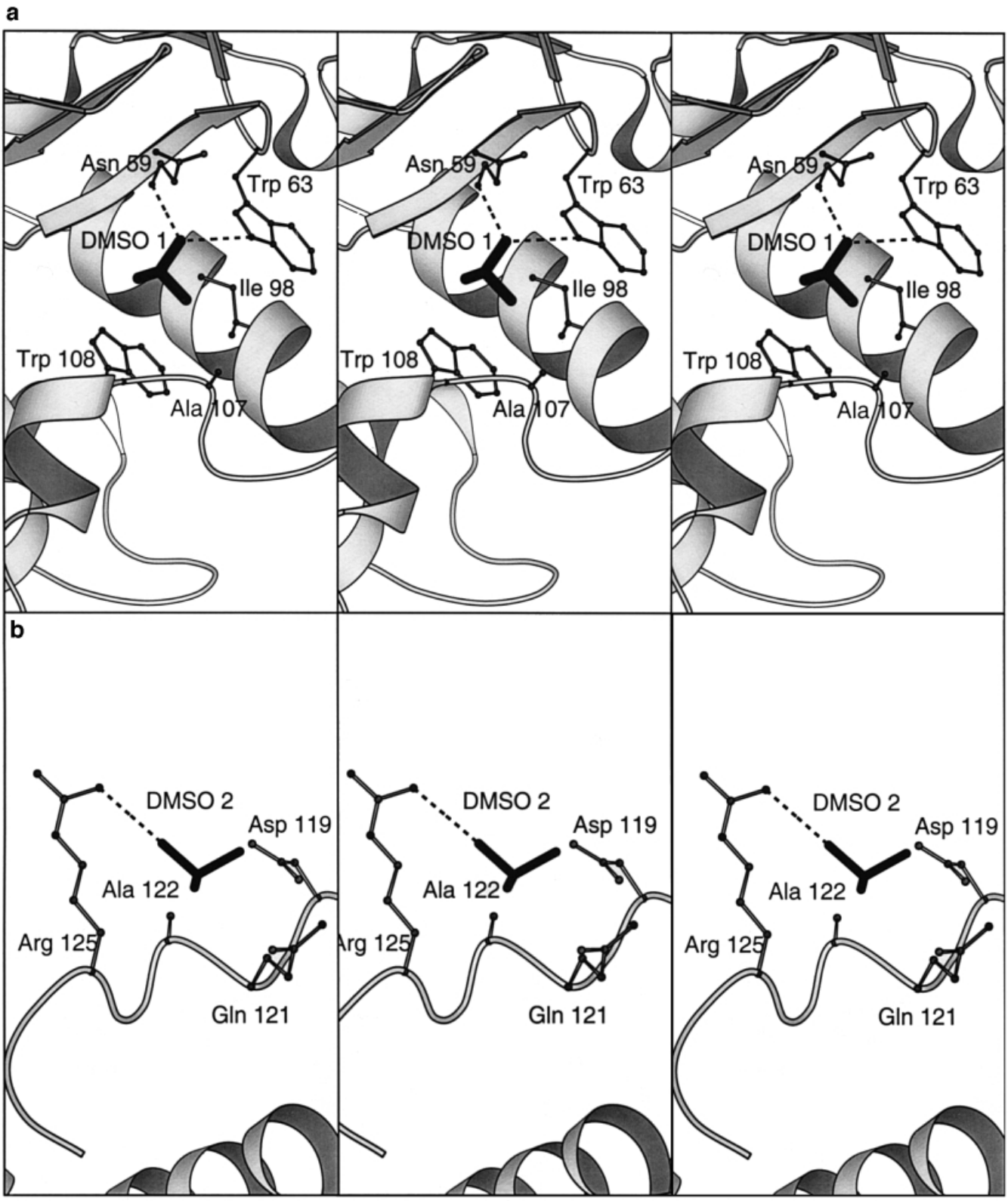

Fig. 3. Binding and interaction of DMSO molecules with HEWL. (**a**) Stereo view of the primary binding site. The binding of this DMSO molecule is in the C-subsite of the carbohydrate binding cleft. The sulfur atom points away from the protein moiety, in agreement with the neutron crystallography data (Lehmann and Stansfield, 1989), but in contrast to the NMR data (Liepinsh and Otting, 1997). (**b**) Binding of the DMSO in a small cleft on the protein surface.

The largest shift in side chain coordinates occurs for Ser72 by 1.81 Å in the DMSO complex, and by 1.96 Å in the GnCl complex. The large shift in Ser72 partly accommodates the disorder and the peptide flip in Arg73. Side chains involved in interactions with the denaturants show large deviations in both the complexes. The Trp62 side chain also exhibits a large

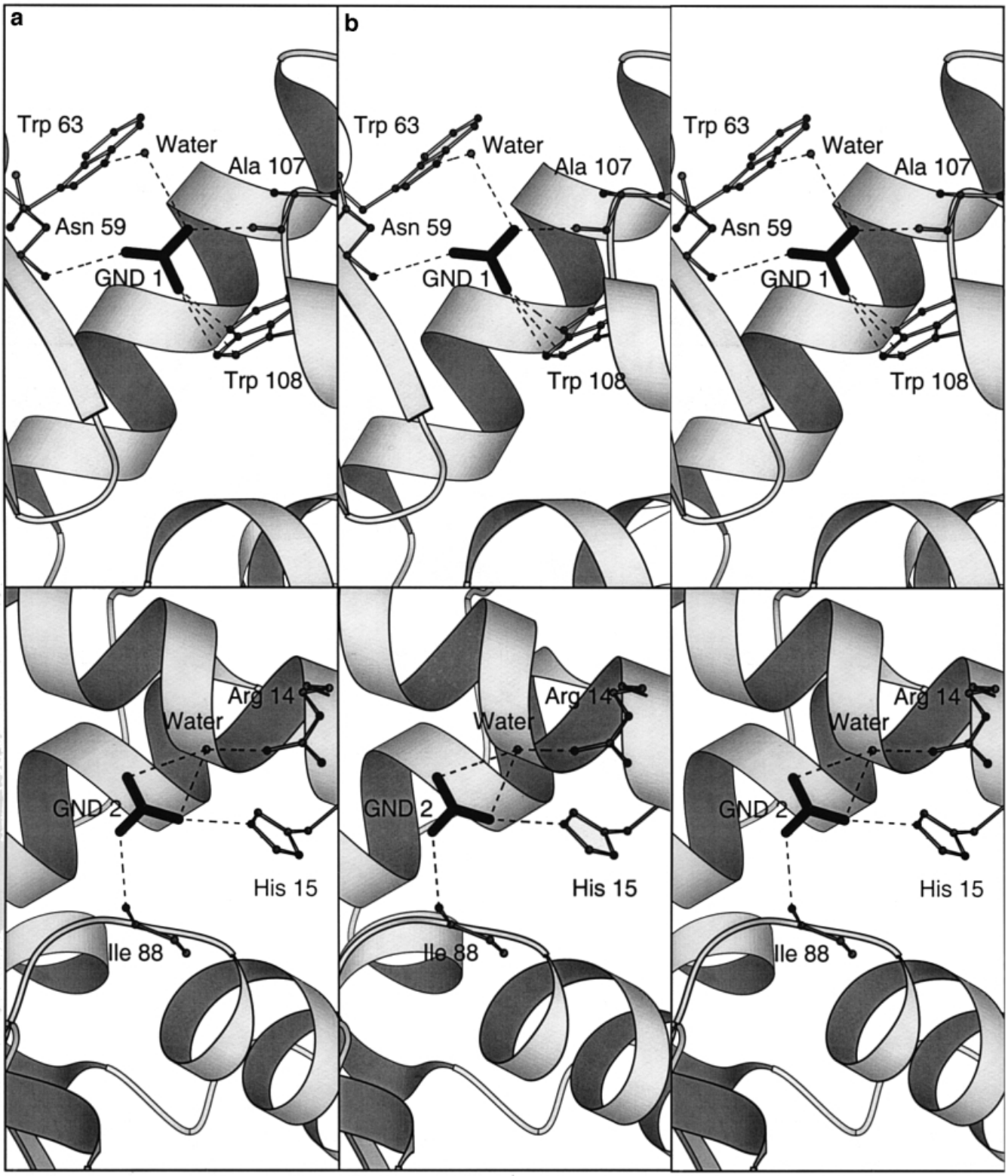

Fig. 4. Geometry of guanidinium ion interaction with HEWL. (**a**) Stereo view of binding in the primary C-site of HEWL. This Gnd ion exhibits interesting interactions with the π electron cloud of Trp108. (**b**) Gnd ion binding to His15, Ile88 and water mediated interaction with Arg14.

shift, as has been characteristically observed in lysozyme sugar complexes (Cheetham *et al*., 1992). The r.m.s. shift in Trp62 side chain coordinates was 1.21 Å in the DMSO complex, while it was 0.73 Å in the GnCl complex.

Some other side chains which exhibit noticeable movement in the complex structures include Arg14 and His15 in the GnCl complex, and Arg45, Val109 and Arg112 in the DMSO complex. In the GnCl complex, His15 flips around its χ^2 dihedral angle thus giving a 180° opposite orientation to its imidazole. The imidazole flip is the direct result of a Gnd ion binding, and also produces a small change in the orientation of the Arg14 side chain. The change in the His15 imidazole

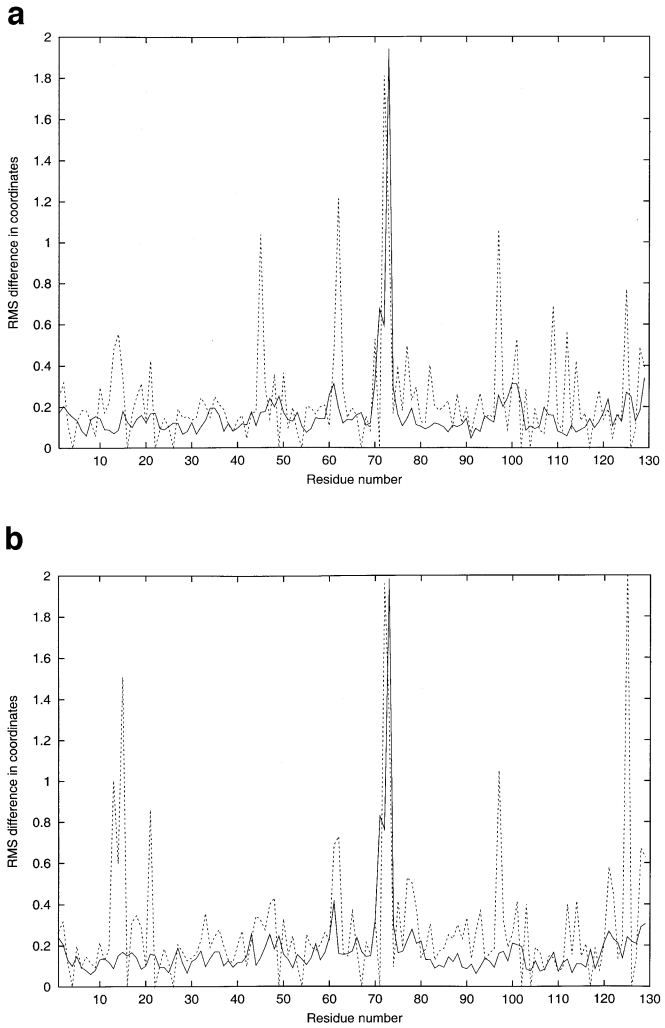

Fig. 5. R.m.s. displacement of residues from the native structure. Displacement for the (**a**) DMSO and (**b**) GnCl complexes. In the both the figures, the solid line represents displacement of the main chain, while the dotted line represents the displacement in the side chain. In both the structures, Ser72 exhibits the largest movement in the side chain.

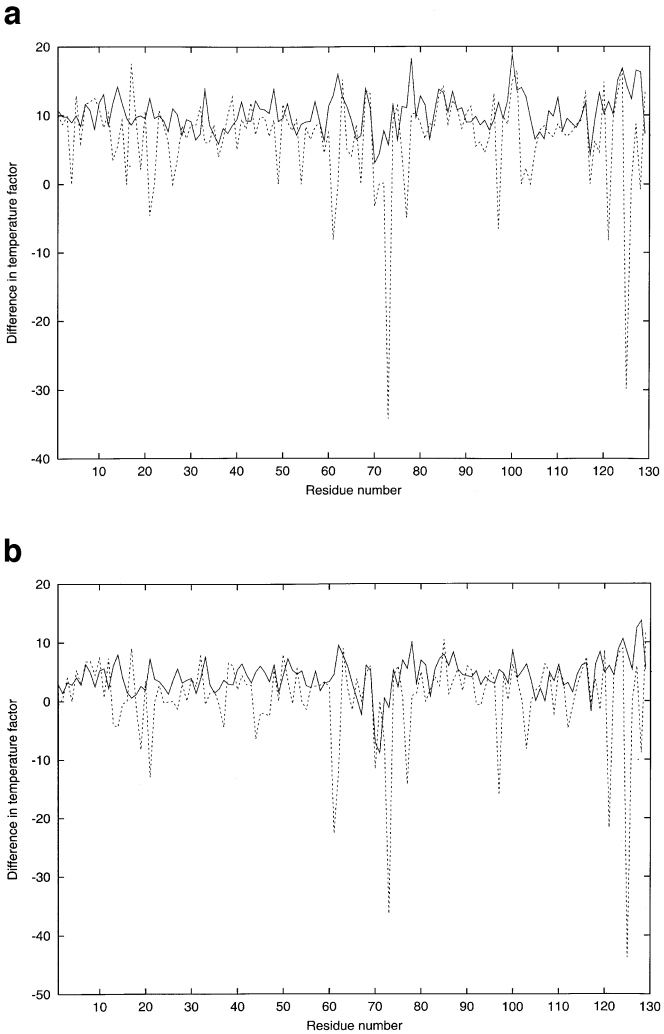

Fig. 6. The difference in temperature factors plotted as a function of residue number. Differences for the (**a**) DMSO and (**b**) GnCl complexes. In both the figures, the solid line represents the average difference in temperature factor for the main chain, while the dotted line represents that for the side chain. The most dramatic difference is observed for residues 72–73, where a noticeable ordering of the structure is observed.

orientation also leads to a loss of its hydrogen bonding interactions with residues Thr89 and Ala11. Similarly, in the DMSO complex, the side chain of Val109 moves to accommodate a DMSO molecule. The movement in Val109 further causes a movement in the side chain of Arg112, breaking its hydrogen bonding interaction with Asn106 (Figure 7). The other major conformational change in the DMSO complex involves Arg45 side chain and results in the loss of hydrogen bonding interactions between Arg45 and a crystal symmetry related Asn44.

Role of a sodium ion

A novel feature of this study was the identification of a Na^+ ion binding site in the lysozyme structure. The overall binding site geometry of Na^+ was the same in both of the complexes (Figure 1). The six ligating atoms are the main chain carbonyl oxygens of residues Ser60, Cys64, Arg73, O^{γ} of Ser72 side chain, and two water molecules. However, due to the disorder in the main chain at Arg73 in the DMSO complex, the Na^+ ion shows only partial occupancy, as evidenced by its higher temperature factor of 31 $Å^2$ (Table II). Moreover, the sixth ligating water molecule of the Na^+ ion was absent in the DMSO complex. On the other hand, the Na^+ site was fully occupied in the guanidinium complex, with a temperature factor of 13.3 $Å^2$ (Table II). Distances between the Na^+ ions and ligating oxygens ranged from 2.6 to 2.8 Å. The sodium ion binding site has not been observed in any of the other HEWL structures to the best of our knowledge. Its creation is partly a consequence of the flipping of the 73–74 peptide bond. It is interesting to note that even in the urea complex, HEWL does not generate a Na^+ binding site despite flipping of the same peptide bond (Pike and Acharya, 1994). Apart from the main chain peptide flip, since side chain movements, notably of Ser72, appear to be crucial in creating the Na^+ ion binding site, it may be assumed that conformational change in the urea complex is not sufficient for the proper binding of Na^+. Alternatively, the sixth ligating water may prove to be crucial for the generation of a Na^+ binding site, lack of which partially destabilizes the Na^+ position in the present DMSO complex.

The Na^+ ion binds lysozyme in the long loop at the interface of the α and β domains. The long loop is known to be an inherently flexible (Madhusudan and Vijayan, 1991) feature of the structure. However, in both our complexes the loop

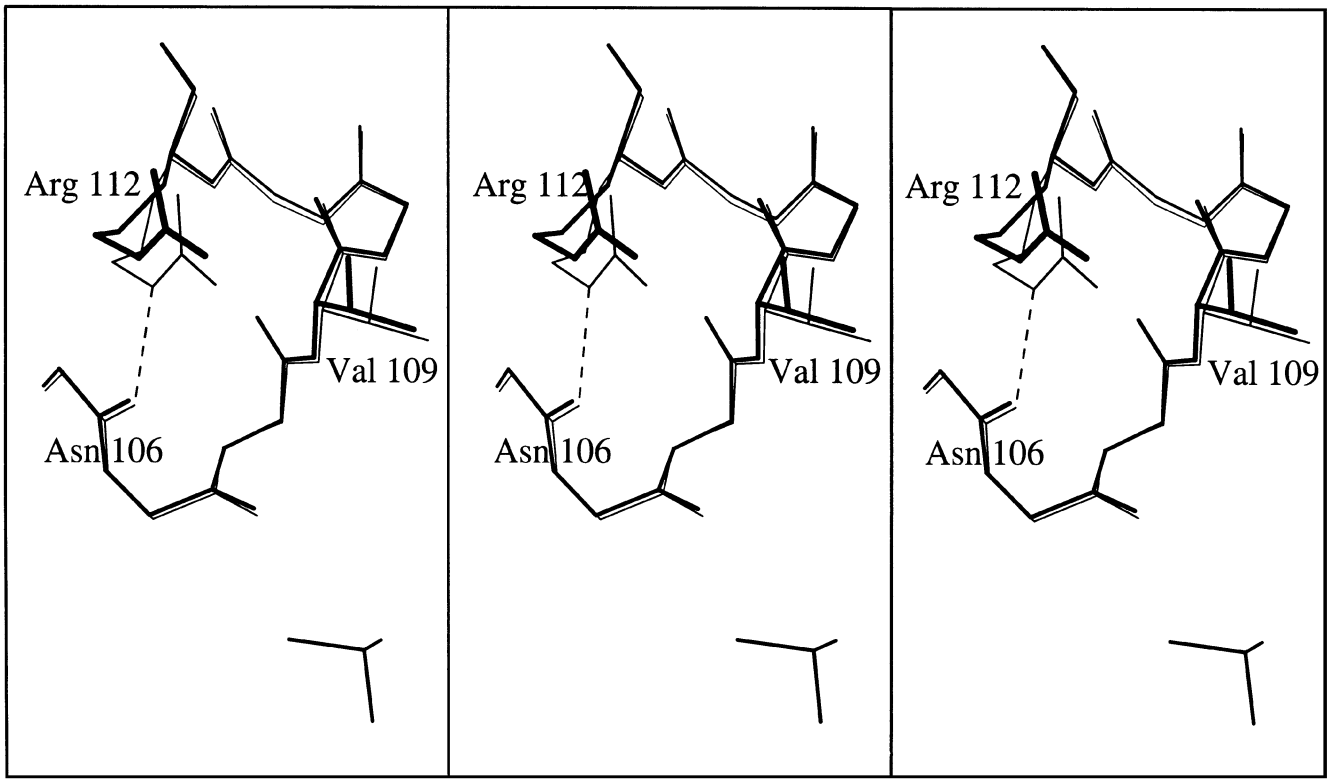

Fig. 7. Stereo view of the side chain conformational difference induced by DMSO binding. The native structure is shown in thin lines, while the DMSO complex is shown in thick lines. A movement in Val109 prompts Arg112 to move farther than its native position. This results in the loss of a hydrogen bond between the Arg112 side chain and the main-chain carbonyl oxygen of Asn106. See text for further details.

conformation is stabilized due to Na^+ binding as evidenced by a dramatic drop in temperature factors (Figure 6a and b).

Discussion

Protein denaturant interactions is an important area of study and their visualization may permit understanding the early events of protein unfolding (Dobson *et al*., 1994). Some of the earlier studies on crystallographic analysis of protein denaturant complexes have identified specific sites on protein surfaces for the binding of denaturant molecules (Dunbar *et al*., 1997; Ratnaparakhi and Varadarajan, 1997). In addition to crystallographic analysis, NMR studies (Neri *et al*., 1992; Liepinsh and Otting, 1997) and calorimetric studies (Makhatadze and Privalov, 1992) have also provided useful insights into such interactions.

In the present study, we have attempted to structurally characterize the complexes of HEWL with DMSO and GnCl, both the compounds known to unfold the protein at sufficiently high concentrations. Some of our observations arising out of this study are, however, at variance with earlier similar studies using different model proteins. For example, other studies point out the importance of an overall decrease in thermal parameters in the presence of denaturants (Pike and Acharya, 1994; Dunbar *et al*., 1997), whereas in both our complexes we find an increase in the mean B-factors. Unfortunately, since the B-factors represent both static as well as dynamic disorder, it is difficult to ascertain at present whether the increase was due to the effect of denaturants or not. The absence of denaturant binding sites at the crystal packing interfaces suggests that the worsening of crystal quality may not be a consequence of denaturant binding. Large movement in the Arg45 side chain, as observed in the DMSO complex, and the consequent loss of an intermolecular interaction with Asn44 may suggest that the deterioration in crystal quality was the result of conformational changes in the protein. Moreover, since the crystal quality became progressively poorer with higher concentrations of denaturant, and the crystals on which data were collected contained maximum permissible denaturant concentration, it is tempting to suggest that the disorder may be due to increased dynamics.

The number of DMSO binding sites observed in our studies were far less than those observed by neutron crystallography (Lehmann and Stansfield, 1989). This was presumably due to the differences in packing interactions between the tetragonal form used in this study and the triclinic form used in neutron crystallography. As many as four out of the six observed DMSO molecules located by neutron diffraction were seen to be involved in crystal contacts. None of these four molecules were observed in our structure, thus strongly suggesting that they indeed non-covalently cross-link the symmetry-related lysozyme molecules in the triclinic crystal form. On the other hand, the DMSO binding sites observed in our complexes were not involved in any crystal contacts, and may perhaps represent the natural binding sites of DMSO. It is pertinent to note that at least one of the DMSO binding sites observed in our complex was the same as that seen in the neutron diffraction experiment (Lehmann and Stansfield, 1989).

The mean temperature factor deviation from the native lysozyme observed by neutron crystallography in the DMSO complex does not show as dramatic a change as seen in our complex. Particularly, the significant temperature factor drop for residues 72 and 73, as well that for many side chains was

not seen in the neutron crystallography data. More significantly, the peptide flip which was observed even in the urea complex (Pike and Acharya, 1994), was not seen in the neutron crystallography data (Lehmann and Stansfield, 1989). Since the region 65–75 is known to be inherently flexible in the HEWL structure (Madhusudan and Vijayan, 1992), we do not believe that the flip was due either to crystallization artifacts, or to differences in packing interactions.

A novel finding of our study was the generation of a Na^+ binding site in the presence of both the denaturants. The sodium ion enjoys a nearly perfect octahedral coordination in the GnCl complex (Figure 2), while due to its lower occupancy in the DMSO complex, does not seem to have a sixth liganding partner. The binding of sodium is greatly facilitated by the 73–74 peptide flip, and a concomitant movement of the side chains in its neighbourhood. Although the peptide flip has been observed in the HEWL–urea complex, perhaps the binding site could not be created due to the lack of movement in the side chains in the urea complex. Interestingly, HEWL is resistant to denaturation by urea, while it can be unfolded using both DMSO and GnCl. The sodium binding in our complexes, and not in any other HEWL structure, was therefore most intriguing.

It has been reported from comparative tryptophan fluorescence analysis of refolding HEWL using GnCl and DMSO that burial of tryptophan residues takes place faster if the protein is refolded from the DMSO denatured state (Kotik *et al*., 1995). A possible explanation for this can be offered from the crystallographic analysis in terms of differences of interactions between the two denaturants with tryptophan residues of HEWL. Our findings show that Gnd ions interact extensively with the Trp residues through their π electrons, and also through direct as well water mediated hydrogen bonding. The DMSO molecule, on the other hand, makes only one hydrogen bond with N^{ε} of tryptophan. Therefore, solvation of a free tryptophan is perhaps energetically more favourable with Gnd ions than with DMSO molecules. Consequently, displacement of denaturant molecules from the fluorescent tryptophans may be slower for Gnd ions than DMSO molecules, and hence the change in rate of folding.

Side chain–main chain interactions provide a critical stabilizing influence on the folded conformation of proteins, and loss of such interactions perhaps form the initial events of protein unfolding. The side chain conformational perturbations observed in both our complexes suggest interesting possibilities for the early events of unfolding. The flipping of His15 imidazole in the GnCl complex, and the movement of the Arg112 side chain in the DMSO complex both provoke tempting speculations. Conformational change in the His15 and Arg112 side chains both lead to loss of side chain–main chain interactions, and are clearly attained due to denaturant binding. The His15 imidazole flipping is in excellent agreement with an earlier NMR observation that local structure in the vicinity of His15 is not very stable (Laurents and Baldwin, 1997). The loss of His15:Thr 89 and His15:Ala11 hydrogen bonding interactions present in the native structure is clearly brought about by the binding of Gnd ions. The destabilization of local structure in the neighbourhood of His15 was, however, not observed in the DMSO complex. Similarly, the loss of the Arg112:Asn106 hydrogen bond observed in the DMSO complex does not occur in the GnCl complex. Such side chain motions may therefore be an effect of the denaturant character. This should provide further impetus to the study of how the loss of side chain–main chain interactions leads to local unfolding by specific denaturants.

Our crystallographic analysis of DMSO and GnCl interactions with HEWL thus shows that the denaturants bind in a characteristic manner to the protein. Although the overall temperature factor of the protein appeared to increase, presumably due to an increased dynamic mobility, there were dramatic reductions in the mobility in parts of the protein. Both the denaturants can induce a Na^+ binding site in the protein, although to different extents. It remains to be seen if Na^+ binding is specifically generated for other disruptants of protein structure.

Acknowledgements

We thank Dinakar Salunkhe for access to the MAR research imaging plate detector for diffraction data collection and Eleanor Dodson for useful suggestions and hints during refinement. We also thank Sagar Nimsadkar for help in crystallizations, the protein design group of IMTECH for stimulating discussions, and Sharmila Mande and K.V.Radhakishan for critical reading of the manuscript. E.S. is a CSIR research associate. Financial support for the work was provided by IMTECH and CSIR.

References

Alderton,G., Ward,W.H. and Fevold,H.L. (1945) *J. Biol. Chem.*, **157**, 43–58.
Breslow,R. and Guo,T. (1990) *Proc. Natl Acad. Sci. USA.*, **87**, 167–169.
Buck,M. (1998) *Q. Rev. Biophys.*, **31**, 297–355.
Burley,S.K. and Petsko,G.A. (1988) *Adv. Protein Chem.*, **39**, 125–189.
Cheetham,J.C., Artymiuk,P.J. and Phillips,D.C. (1992) *J. Mol. Biol.*, **224**, 613–628.
Collaborative Computational Project, Number 4 (1994) *Acta Crystallogr.*, **D50**, 760–763.
Dobson,C.M., Evans,P.A. and Radford,S.E. (1994) *Trends Biochem. Sci.*, **19**, 31–37.
Dunbar,J., Yennawar,H.P., Banerjee,S., Luo,J. and Farber,G.K. (1997) *Protein Sci.*, **6**, 1727–1733.
Jones,T.A., Zou,J.Y., Cowan,S.W. and Kjeldgaard,M. (1991) *Acta Crystallogr.*, **A47**, 110–119.
Kodandapani,R., Suresh,C.G. and Vijayan,M. (1990) *J. Biol. Chem.*, **265**, 16126–16131.
Kotik,M., Radford,S.E. and Dobson,C.M. (1995) *Biochemistry*, **34**, 1714–1724.
Kraulis,P.J. (1991) *J. Appl. Crystallogr.*, **24**, 946–950.
Kundrot,C.E. and Richards,F.M. (1987) *J. Mol. Biol.*, **193**, 157–170.
Laskowski,R.A., MacArthur,M.W., Moss,D.S. and Thornton,J.M. (1993) *J. App. Crystallogr.*, **26**, 283–290.
Laurents,D.V. and Baldwin,R.L. (1997) *Biochemistry*, **36**, 1496–1504.
Lehmann,M.S., Mason,S.A. and McIntyre (1985) *Biochemistry*, **24**, 5862–5869.
Lehmann,M.S. and Stansfield,R.F.D. (1989) *Biochemistry*, **28**, 7028–7033.
Liepinsh,E. and Otting,G. (1997) *Nature Biotechology*, **15**, 264–268.
Madhusudan and Vijayan,M. (1991) *Curr. Sci.*, **60**, 165–170.
Madhusudan and Vijayan,M. (1992) *Protein Engng*, **5**, 399–404.
Makhatadze,G.I. and Privalov,P.L. (1992) *J. Mol. Biol.*, **226**, 491–505.
Murshudov,G.N., Vagin,A.A. and Dodson,E.J. (1997) *Acta Crystallogr.*, **D53**, 240–255.
Neri,D., Billeter,M., Wider,G. and Wuthrich,K. (1992) *Science*, **257**, 1559–1563.
Otwinowski,Z.O. and Minor,W. (1997) In Carter,C.W. and Sweet,R.M. (eds) *Methods Enzymol.*, **276**, 307–326.
Pike,A.C.W. and Acharya,K.R. (1994) *Protein Sci.*, **3**, 706–710.
Ratnaparkhi,G.S. and Varadarajan,R. (1997) *Curr. Sci.*, **72**, 826–830.
Snape,K.W., Tjian,R., Blake,C.C.F. and Koshland,D.E. (1974) *Nature*, **250**, 295–298.
Tanford,C. (1968) *Adv. Protein Chem.*, **247**, 1708–1712.
Thayer,M.M., Hailtwanger,R.C., Allured,V.S., Gill,S.C. and Gill,S.J. (1993) *Biophys. Chem.*, **46**, 165–169.
Young,A.C.M., Tilton,R.F. and Dewan,J.C. (1994) *J. Mol. Biol.*, **235**, 302–317.

Received June 9, 1999; revised November 18, 1999; accepted December 8, 1999